유한체적법을 이용한 제방붕괴 해석

Numerical Analysis of Embankment Failure with Finite Volume Method

유재홍*, **김형준****, **조용식*****

Jae Hong Yu, Hyung Jun Kim, Yong-Sik Cho

Abstract

홍수범람은 무제부에서의 하천수위 상승으로 인해 제내로 서서히 침수해가는 것과 월류로 인한 제방의 파괴를 동반하는 급격한 범람의 두 가지 형태가 있다. 기존연구들은 대부분이 월류에 의한 제방붕괴를 고려할 경우, 제방붕괴가 점진적으로 발생함에도 불구하고 이를 수치모형에 적용할 경우 갑작스럽게 지형을 낮추거나 초기지형으로써 제방붕괴를 가정하여 이를 고려해왔다. 본 연구에서는 제방붕괴를 시간의존적인 함수로 가정하고 이를 고려할 수 있는 서브프로그램의 개발을 통해 기존의 방법과 비교하여 그 영향을 검토하였다.

본 연구에 사용된 수치모형은 비선형의 2차원 천수방정식을 비구조적 격자계가 적용된 유한체적법을 이용하였으며, Riemann 해를 계산하기 위하여 approximate HLLC Riemann solver를 이용하였다. 기연구된 제방붕괴 고려방법과 본 연구의 시간의존적인 제방붕괴 고려방법을 통해 월류량을 비교하였을 때, 기존연구들의 홍수범람 해석결과가 과다예측 되었음을 알 수 있었다. 추후의 이루어질 연구들에서는 시간의존적인 제방붕괴를 반드시 고려해야됨과 동시에 이를 자연현상과 좀더 가깝고 효과적으로 고려할 수 있도록 연구가 필요하다.

핵심용어 : 제방붕괴, 유한체적법, 시간의존적, approximate HLLC Riemann solver

1. Introdution

Embankments and flood protection walls are designed to protect human reigns and property from the flood inundation. However, in case of the resulting flood wave implicates an extra risk to people and property in the near field of the breach because of the strong dynamic forces. Due to the rareness and dangerousness of such a failure, data from real-world incidents are insufficient to base a prediction of the flood wave propagation on these.

The flood wave propagation can be caused by dam-break flows or embankment-break flows. Most physical investigations took place in flumes and therefore reduced the problem to a one dimensional problem, namely, the propagation takes place only along the flume, lateral propagation is not considered and breach and reservoir have the same width. Only few investigations allowed for a propagation into an area, combined with a breach width smaller than the width of the reservoir.

Physical tests concerning the propagation of the flood wave into an area were proceeded by Kim (1997), Fraccarollo and Toro (1995) and Jovanovic and Djordjevic (1995). All of these authors considered dam-break, but not embankment-break. Aureli and Migmosa (2002) presented the single investigation also taking into account the river discharge. They are performing computations of the levee-break induced wave, while taking measurements in the channel.

* 정회원 · (주)세일종합기술공사 항만부 · E-mail : y2kzone@hanmail.net

** 정회원 · 한양대학교 토목공학과 박사과정 · E-mail : john0705@ihanyang.ac.kr

*** 교신저자 · 한양대학교 토목공학과 교수 · E-mail : ysc59@hanyang.ac.kr

2. Governing Equation

The nonlinear shallow-water equations in a conservative form including slope and frictional effects may be adequate to describe the behaviors of a two-dimensional flow problems. These equations can be written as

$$\frac{\partial \mathbf{U}}{\partial t}+\frac{\partial \mathbf{E}}{\partial x}+\frac{\partial \mathbf{F}}{\partial y}=\mathbf{S} \tag{2.1}$$

in Eq. (2.1), **U** is the conserved vector variables, **E** and **F** are the flux vector functions in x- and y-axis directions, respectively, and **S** is the source terms.

The vectors of **U**, **E**, **F** and **S** can be written as

$$\mathbf{U}=\begin{bmatrix} h \\ hu \\ hv \end{bmatrix}, \mathbf{E}=\begin{bmatrix} hu \\ hu^2+\frac{1}{2}gh^2 \\ huv \end{bmatrix}$$

$$\mathbf{F}=\begin{bmatrix} hv \\ huv \\ hv^2+\frac{1}{2}gh^2 \end{bmatrix}, \mathbf{S}=\begin{bmatrix} 0 \\ gh(S_{ox}-S_{fx}) \\ gh(S_{oy}-S_{fy}) \end{bmatrix} \tag{2.2}$$

where h is the total water depth defined as the sum of a still water depth and free surface displacement, u and v are the velocity components in x- and y-axis directions, g is the acceleration due to gravity. And, S_{ox}, S_{oy}, S_{fx} and S_{fy} are bed slope and bottom friction terms in x- and y-directions, respectively.

The bottom friction terms S_{fx} and S_{fy} have been estimated by using the Manning's empirical formula given as

$$S_{fx}=\frac{un^2\sqrt{u^2+v^2}}{h^{4/3}}, \quad S_{fy}=\frac{vn^2\sqrt{u^2+v^2}}{h^{4/3}} \tag{2.3}$$

in which n is the Manning's roughness coefficient.

For larger systems, such as the Euler equations or the two-dimensional shallow-water equations, the solution to the Riemann problem consists of three waves separating four constant states as described in Fig 2.1 and Fig 2.2, Therefore, the assumption of the HLL approach that two waves separated by three constants is incorrect. In view of these shortcomings of the HLL approach, a modification called the HLLC approximation Riemann solver was put forward by Toro et al. (1994).

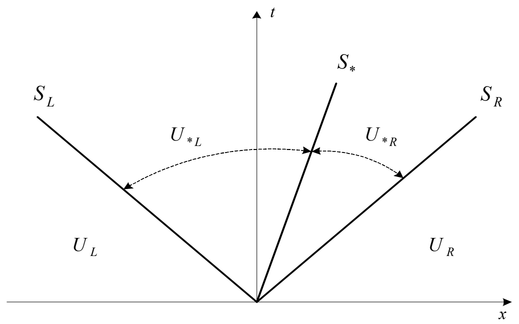

Fig 2.1 Approximate HLLC Riemann solver

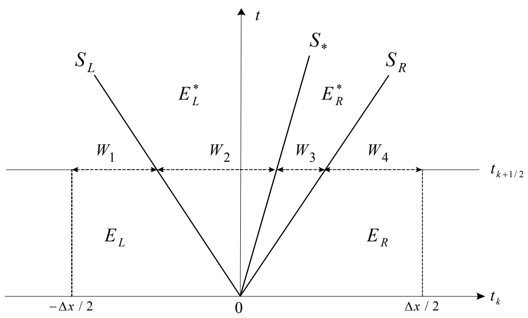

Fig 2.2 Numerical Flux and WAF scheme

The approximate HLLC Riemann solver is given as

$$\tilde{\mathbf{U}}(x,t)=\begin{cases} \mathbf{U}_\mathrm{L} & \text{for } 0 \leqq S_L \\ \mathbf{U}_L^* & \text{for } S_L \leqq 0 \leqq S_* \\ \mathbf{U}_R^* & \text{for } S_* \leqq 0 \leqq S_R \\ \mathbf{U}_\mathrm{R} & \text{for } S_R \leqq 0 \end{cases} \tag{2.4}$$

In order to determine numerical fluxes in the HLLC Riemann solver, the wave speeds in Eq. (2.4) should be estimated. The estimated wave speeds, in this study, are given as

$$\begin{aligned} S_L &= \min(u_L - \sqrt{gh_L}, u_* - \sqrt{gh_*}) \\ S_* &= u_* = \frac{u_L + u_R}{2} + \sqrt{gh_L} - \sqrt{gh_R} \\ S_R &= \max(u_L + \sqrt{gh_L}, u_* + \sqrt{gh_*}) \end{aligned} \tag{2.5}$$

In the view of Eq. (2.4), the HLLC flux can be written as

$$\mathbf{E}_{i+1/2}^{HLLC} = \begin{cases} \mathbf{E}_L & \text{for } 0 \leqq S_L \\ \mathbf{E}_L^* = \mathbf{E}_L + S_L(\mathbf{U}_L^* - \mathbf{U}_L) & \text{for } S_L \leqq 0 \leqq S_* \\ \mathbf{E}_R^* = \mathbf{E}_R + S_R(\mathbf{U}_R - \mathbf{U}_R^*) & \text{for } S_* \leqq 0 \leqq S_R \\ \mathbf{E}_R & \text{for } S_R \leqq 0 \end{cases} \tag{2.6}$$

in which the subscript $i+1/2$ means an intercell boundary between L and R.

3. Analysis of Embankment Failure

3.1 Dam-break Induced Flow

Kim (1997) performed the laboratory experiment to investigate the progress of embankment failure. By the Kim's research, the embankment failure is progressing like Fig 3.1. But, in the numerical model, it is impossible to consider similarly the embankment failure of natural phenomenon. So, we considered various collapse function as simplified the embankment failure mathematically.

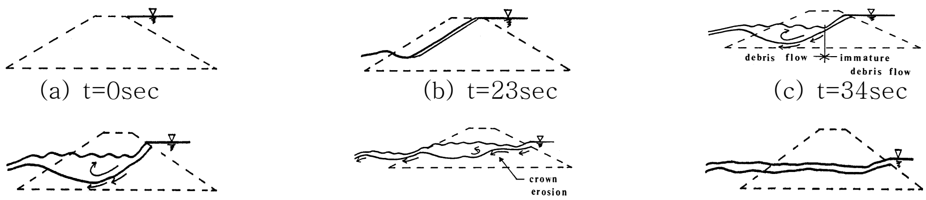

(a) t=0sec (b) t=23sec (c) t=34sec

(d) t=74sec (e) t=121sec (f) t=151sec

Fig 3.1 Timehistory of collapse aspects

Eq. (3.1) is the simplified collapse function. where, $\rho = 0 \sim 3$, t is the processing time after the collapse, T is the duration time of collapse, h_t is the embankment height of arbitrary time, h_I is the initial embankment height and h_F is the final embankment height.

$$h_t = \begin{cases} (h_I - h_F)\left(\frac{t}{T}\right)^{\rho} & \text{for } 0 \leqq t \leqq T \\ h_F & \text{for } t > T \end{cases} \tag{3.1}$$

In this study, CASE 1~3 is $\rho = 1 \sim 3$ and CASE 4 is $\rho = 0$, CASE 4 is the general method to consider the embankment failure for the flood inundation analysis.

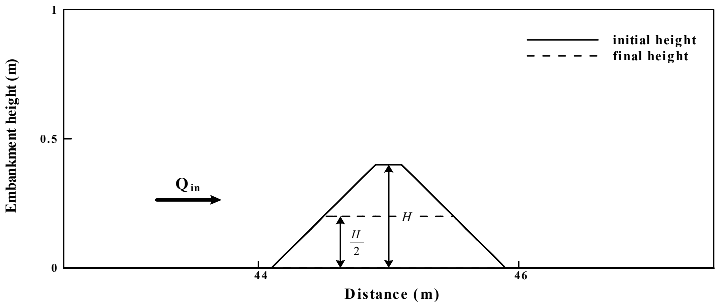

Fig 3.2 Numerical setup of embankment

In Fig 3.2, for numerical model, the section of embankment refer to the constructed embankment of along the domestic river. the top of embankment length is $0.2m$, the initial embankment height is $0.4m$, the final embankment height due to collapse is, a half of initial ones, $0.2m$, the slope of embankment is $1:2$ and total duration time T is $120\sec$.

Fig 3.3~3.6 show the overflow discharge due to inflow discharge. In CASE 4, overflow discharge is always lager than other CASE, because CASE 4 is rapid processing the collapse with the overflow of embankment simultaneously. Table 3.1 shows the overflow discharge for each inflow discharge and CASE. In Table 3.1, the discharge ratio mean the ratio of maximum discharge to minimum discharge in the same inflows. In CASE 4, overflow discharge has more 60% which is amount of in CASE 3, but CASE 1~3 are have a difference slightly. In addition to, numerical results show that as the inflow discharge is increasing, the amount of overflow discharge is decreasing.

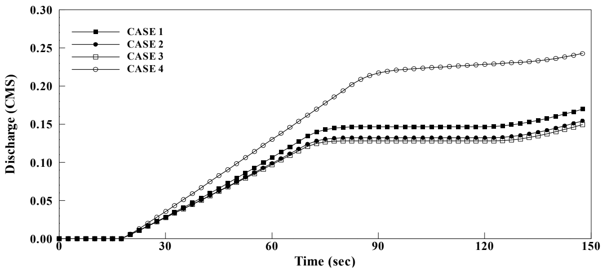

Fig 3.3 Overflow discharge (Q=0.2CMS)

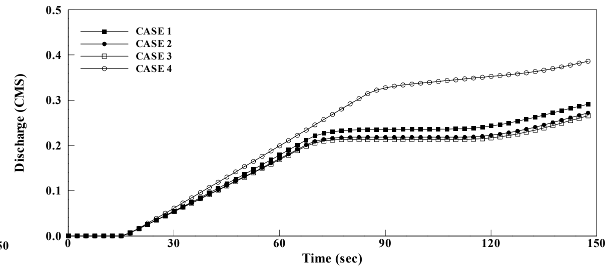

Fig 3.4 Overflow discharge (Q=0.5CMS)

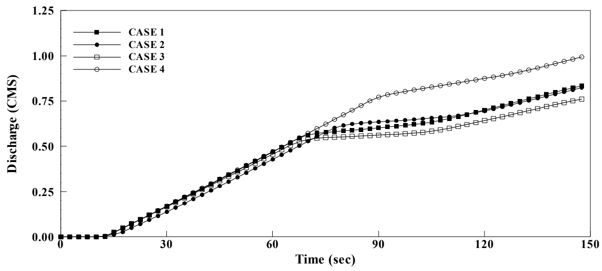

Fig 3.5 Overflow discharge (Q=1.0CMS)

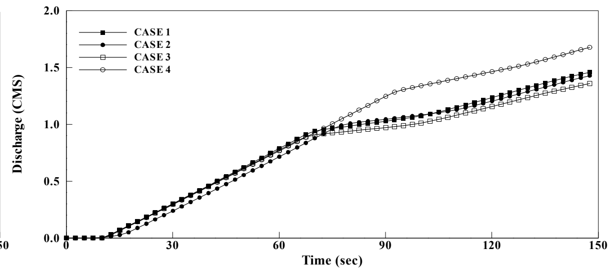

Fig 3.6 Overflow discharge (Q=1.5CMS)

Table 3.1 Comparison of overflow discharge

Description	0.2 CMS	0.5 CMS	1.0 CMS	1.5 CMS
CASE 1	0.173	0.296	0.845	1.476
CASE 2	0.158	0.277	0.836	1.445
CASE 3	0.153	0.271	0.770	1.376
CASE 4	0.245	0.390	1.006	1.700
Discharge Ratio(%)	60.0%	44.0%	30.7%	23.4%

3.2 Embankment-break Induced Flow

To simulate the embankment failure, we made a arbitrary topography as shown Fig 3.7. A embankment is located along the flow direction and its section is equal to in chapter 3.1 ones. In this chapter, we considered both the collapse depth and the collapse width. The collapse duration time and collapse height are same values as in chapter 3.1, but the collapse function assumed only linearly.

To determine the failure width, we refer to the collapse aspects of fill dam. In Table 3.2, shows the collapse width and collapse time and H is the embankment height. In this study, we taken the 3H for the collapse width.

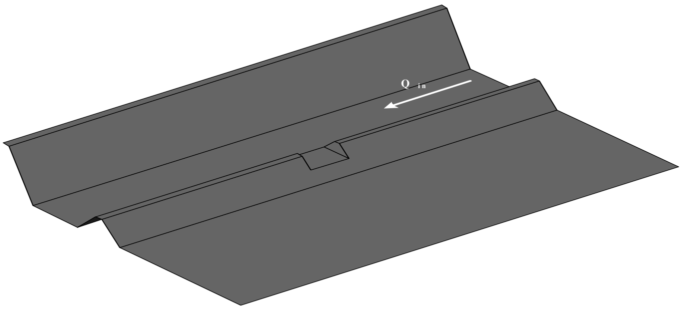

Fig 3.7 Imaginary imulation Topography

Table 3.2 Collapse aspects

	Average collapse width	Collapse time (hr)
Singh	2H≤B≤5H	0.1≤T≤0.5 or 0.5≤T≤3.0
MacDonald	H≤B≤5H	
Fread	H≤B≤3H	

The initial water depth is $0.15m$ along the channel and the inflow discharge is 0.3CMS in all cases. Table 3.3 shows the cases descriptions. CASE 1 is the general method to simulate the embankment failure in flood inundation analysis and CASE 2~4 are time-dependent method suggested in this study.

Table 3.3 CASE description

Description	Height variation	Width variation
CASE 1	rapid decrease	rapid increase
CASE 2	linearly decrease	rapid increase
CASE 3	rapid decrease	linearly increase
CASE 4	linearly decrease	linearly increase

In Fig 3.8 shows the total overflow discharge due to the CASE. The overflow discharge shows the largest in CASE 1 and CASE 4 is the smallest. In CASE 1, the overflow is started at $t=5\text{sec}$, CASE 2 is $t=12\text{sec}$, CASE 3 is $t=7\text{sec}$ and CASE 4 is $t=20\text{sec}$. CASE 1 is 5 time larger than CASE 4 in the amount of the total overflow discharge. In a series of obtained results, we can know that the existing studies were overestimated the flooding discharge in the flood inundation analysis. Also, we need the new technique to control the embankment failure effectively and more closely the natural phenomenon.

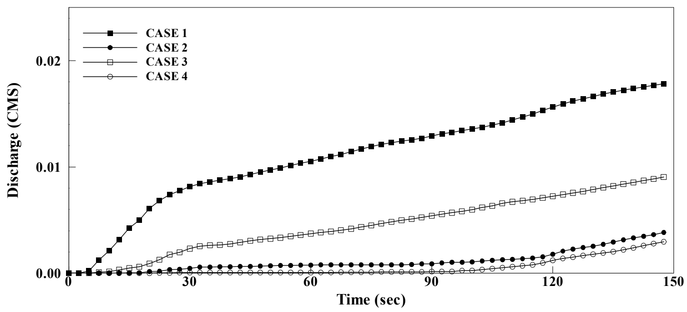

Fig 3.8 Overflow discharge (Q=0.3CMS)

4. Concluding Remarks

In this study, a numerical analysis for the time-dependent embankment -break flows has been performed. The present numerical model based on the shallow-water equations has been applied to the unstructured grid systems. By using a fractional step method, the two-dimensional nonlinear shallow-water equations can be split into two augmented one-dimensional equations along x- and y- axis directions. And the use of the approximate HLLC Riemann solver enables to handle discontinuities such as shock propagations.

In the dam-break induced flow problem, the numerical results of the general method compared with the time-dependent method ones, and the overflow discharge show an 23～60% increment than time-dependent method. The overflow discharge is decreasing as the inflow discharge increasing. In the embankment-break induced flow problem, we are considering the time-dependent variation of collapse width and height, and simulated the many possible cases. The numerical results show that the variation of collapse width more affected on the amount of the flooding discharge, and the flooding discharge of general method are five times as much as the time-dependent method ones. As a sequence of the numerical results, we known that the existing researches of flood inundation analysis are overestimating the flooding discharge.

The aim of this study was to test the capabilities of the numerical model in complex situations in which the underlying assumptions at the basis of the mathematical description may be not completely satisfied. The model can then be adopted to describe rapidly varying flows that could occur in nature, as requested for example in flooding map evaluation for risk assessment.

감사의 글

본 연구는 해양수산부(KGSP)에 의해 지원되었습니다.

참고문헌

1. Aureli, F., Mignosa, P. (2002). "Rapidly varying flows due to levee-breaking." *Proc. International Conference on Fluvial Hydraulics,* 4-6 September, 459-466
2. Fraccarollo, L., Toro, E.F. (1995). "Experimental and numerical assessment of the shallow water model for two-dimensional dam-break type problems." *Journal of Hydraulic Research,* 33(6), 843-863.
3. Jovanovic, M., Djordjevic, D. (1995). "Experimental verification of the MacCormack numerical scheme." *Advances in Engineering Software,* 23, 61-67.
4. Kim, J.-H. (1997). "Hydraulic characteristics of fluid-granule mixed flow in embankment of noncohesive materials due to overflow." *Korea Water Resources Association*, 30(6), 661-669.
5. Toro, E.F., Spruce, M. and Speares, W. (1994). "Restoration of the contact surface in the HLL Riemann solver." *Shock Waves*, 4, 25-34.